Journal of Modern Optics
Vol. 52, No. 16, 10 November 2005, 2197–2205

Taylor & Francis
Taylor & Francis Group

Synthesis of time-bin entangled states via tailored group velocity matching

ALFRED B. U'REN*†‡, REINHARD ERDMANN§ and IAN A. WALMSLEY†

†Clarendon Laboratory, Oxford University, Parks Road, Oxford, OX1 3PU, England
‡Centro de Investigación Científica y Educación Superior de Ensenada (CICESE), Baja California, 22860, Mexico
§Sensors Directorate, Air Force Research Laboratory, Rome, NY

(*Received 15 February 2005; in final form 25 April 2005*)

We show that tailored group velocity matching in non-linear $\chi^{(2)}$ crystal sequences interspersed with birefringent $\chi^{(1)}$ compensators can be used to generate time-bin entangled states. By choosing the crystal and compensator materials appropriately it is possible to generate all four time-bin Bell states without resorting to time non-stationary devices. This scheme, in addition, lends itself well to the generation of higher-dimensionality states such as time-bin qutrits.

Group velocity matching (GVM) in the process of parametric downconversion (PDC) has previously been shown to constitute a powerful tool for tailoring the spatio-temporal structure of generated photon pairs. For example, the group velocity matching condition derived by Keller *et al*. [1] can be used to synthesize spectrally decorrelated states [2] and states with coincident frequencies [3–5]. Unfortunately, group velocity matching is inherently dependent on material dispersion, and therefore tends to occur at specific wavelengths. We have introduced a novel technique based on a *sequence* of crystals interspersed with birefringent compensators which can be used to attain group velocity matching at arbitrary wavelengths [6]. In [6] we have indeed shown that such a technique can be used to engineer the spectral correlations in two photon states to meet specific needs. We have, in addition, demonstrated experimentally that such a technique can be successfully exploited to revert the interference loss resulting from spectral distinguishability in type-II PDC photon pairs [7]. In this paper we present theoretical work indicating that a crystal pair interspersed by a single birefringent medium can be used to generate time-bin Bell states where tailoring of the GVM conditions allows the generation of all four Bell states without the need for time non-stationary devices.

*Corresponding author. Email: auren@cicese.mx

Journal of Modern Optics
ISSN 0950–0340 print/ISSN 1362–3044 online © 2005 Taylor & Francis
http://www.tandf.co.uk/journals
DOI: 10.1080/09500340500275843

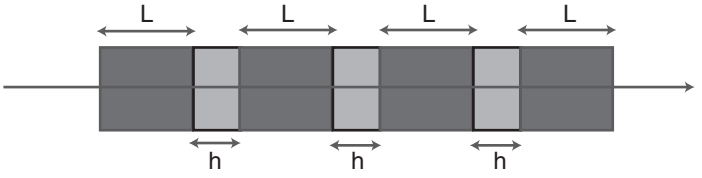

Figure 1. Sequence comprised of N $\chi^{(2)}$ crystals interspersed with $N-1$ birefringent spacers.

We start our analysis by writing the state produced by spontaneous PDC pumped by an ultrashort pulse train for fixed propagation directions [8]:

$$|\Psi\rangle = |0\rangle_s|0\rangle_i + \eta \iint d\omega_s d\omega_i f(\omega_s, \omega_i) a_s^\dagger(\omega_s) a_i^\dagger(\omega_i)|0\rangle_s|0\rangle_i, \tag{1}$$

where η is the PDC process efficiency, $a_\mu^\dagger(\omega_\mu)$ $(\mu = s, i)$ is the frequency-dependent creation operator for the PDC signal(s) and idler(i) modes; and $f(\omega_s, \omega_i)$ is the joint spectral amplitude (JSA), where

$$|f(\omega_s, \omega_i)|^2 = \langle\Psi|a_s^\dagger(\omega_s) a_i^\dagger(\omega_i) a_s(\omega_s) a_i(\omega_i)|\Psi\rangle = |\alpha(\omega_s + \omega_i)\phi(\omega_s, \omega_i)|^2 \tag{2}$$

represents the probability distribution of emitted frequencies (or joint spectral intensity [JSI]) in terms of the pump envelope function (PEF) $\alpha(\omega_s + \omega_i)$ and the phase-matching function (PMF) $\phi(\omega_s, \omega_i)$ [8].

Consider the experimental arrangement shown in figure 1 consisting of N identical $\chi^{(2)}$ crystals of thickness L and $N-1$ identical linear $\chi^{(1)}$ spacers of thickness h. Each of the crystals is assumed to be cut and oriented for degenerate collinear type-II PDC while the spacers are assumed not to exhibit a $\chi^{(2)}$ nonlinearity. The resulting PMF for this structure is given by [6]:

$$\phi_N(\nu_s, \nu_i) = \mathrm{e}^{i/2[N\Delta k(\nu_s, \nu_i)L + (N-1)\Delta\kappa(\nu_s, \nu_i)h]} \frac{\sin((N\Phi(\nu_s, \nu_i))/2)}{\sin(\Phi(\nu_s, \nu_i)/2)} \operatorname{sinc}\left[\frac{L\Delta k(\nu_s, \nu_i)}{2}\right] \tag{3}$$

where we have defined $\Phi(\nu_s, \nu_i) = L\Delta k(\nu_s, \nu_i) + h\Delta\kappa(\nu_s, \nu_i)$ in terms of the crystal phase mismatch $\Delta k = k_p - k_s - k_i$ and spacer phase mismatch $\Delta\kappa = \kappa_p - \kappa_s - \kappa_i$. Hence, apart from a phase factor the crystal assembly PMF is composed of the product of two distinct functions: the single crystal PMF and a contribution which incorporates the combined crystal and spacer dispersion. Using the change of variables $\nu_\pm = 2^{-1/2}(\nu_s \pm \nu_i)$ and carrying out a Taylor expansion of $\Delta k(\nu_s, \nu_i)$ and $\Delta\kappa(\nu_s, \nu_i)$ we obtain:

$$\Phi(\nu_+, \nu_-) = h\Delta\kappa^{(0)} + L\Delta k^{(0)} + \tau_+\nu_+ + \tau_-\nu_-, \tag{4}$$

where $L\Delta k^{(0)}$ and $h\Delta\kappa^{(0)}$ denote the constant Taylor expansion terms and where the first order coefficients are:

$$\begin{aligned} \tau_+ &= 2^{-1/2}\left[L(k_s' + k_i' - 2k_p') + h(\kappa_s' + \kappa_i' - 2\kappa_p')\right] \\ \tau_- &= 2^{-1/2}\left[L(k_s' - k_i') + h(\kappa_s' - \kappa_i')\right]. \end{aligned} \tag{5}$$

Let us specialize our discussion to the case of two crystals interspersed by a single compensator, i.e. $N=2$. Assuming a Gaussian PEF with bandwidth σ, the JSA becomes:

$$f(\nu_+,\nu_-)=\operatorname{sinc}\left[\frac{1}{2}(T_+\nu_+ + T_-\nu_-)\right] \times \cos\left[\frac{1}{2}\left(h\Delta\kappa^{(0)}+\tau_+\nu_+ + \tau_-\nu_-\right)\right]\exp\left[-\frac{2}{\sigma^2}\nu_+^2\right] \tag{6}$$

where we assume that the phase-matching condition $\Delta k^{(0)}=0$ holds and where $T_\pm$ are given by equation (5) with $h=0$. We proceed to analyse the PDC time of the emission probability distribution (or the joint temporal intensity [JTI]):

$$\langle\Psi|a_s^\dagger(t_s)a_i^\dagger(t_i)a_s(t_s)a_i(t_i)|\Psi\rangle=|\tilde{f}(t_s,t_i)|^2 \tag{7}$$

where the joint temporal amplitude (JTA) $\tilde{f}(t_s,t_i)$ represents the Fourier transform of the JSA $f(\omega_s,\omega_i)$. The cosine term in equation (6) yields, upon Fourier transformation, the coherent sum of two distinct photon pair emission amplitudes in the temporal domain (convolved with the transformed PEF and single crystal PMF). The resulting configuration of these two amplitudes on the $\{t_s,t_i\}$ plane is such that: (i) the temporal offset between them is inversely proportional to the cosine modulation frequency on the $\{\omega_s,\omega_i\}$ plane, and (ii) the *direction* of the temporal offset on the $\{t_s,t_i\}$ plane depends on the combined crystal and spacer dispersion. As will be studied in this paper, a two-photon state exhibiting distinct amplitudes temporally offset from each other results in so-called time-bin entanglement.

For type-II PDC where the signal and idler wavepackets are orthogonally polarized and therefore experience different dispersion characteristics, the signal and idler group velocities are, in general, neither matched to each other nor to that of the pump pulse. Here we study two specific types of tailored GVM scenarios possible in a crystal-spacer-crystal sequence: (i) signal to idler GVM and (ii) PDC photon pair to pump pulse GVM. In (i) the two PDC photons remain temporally overlapped upon propagation, while they walk away from the pump pulse. In (ii) the pump pulse remains locked to the mean signal/idler wavepacket instantaneous position, while the signal to idler group delay increases upon propagation. Even though dispersion implies that GVM (of either of the above types) occurs at best at isolated wavelengths, a sequence composed of crystals and birefringent compensators can be used to limit the maximum observed group velocity mismatch (of a given type, according to the desired application) to that observed in a single (thin) crystal segment. Note that the case of full GVM, in which the signal, idler and pump fields remain temporally overlapped upon propagation, is not considered in this paper.

The first GVM scenario described above corresponds to $\tau_-=0$ and requires (see equation 5) (i) $k_s'-k_i'$ and $\kappa_s'-\kappa_i'$ to exhibit opposite signs and (ii) the thicknesses L and h to be chosen appropriately so that $\tau_-=0$. This condition can be fulfilled with a pair of type-II BBO crystals and a quartz spacer: while BBO exhibits $k_e'-k_o'=193.8\,\text{fs/mm}$ (where 'o' and 'e' refer to the ordinary and extraordinary polarizations), quartz exhibits $\kappa_e'-\kappa_o'=-31.8\,\text{fs/mm}$ (at 800 nm);

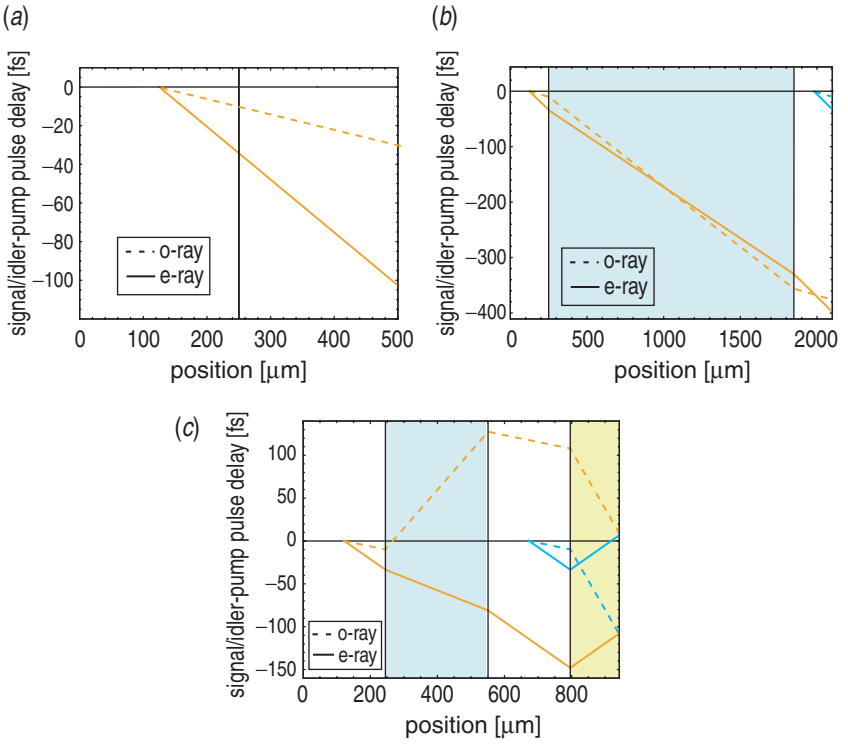

Figure 2. Timing diagram showing the delay between each of the signal and idler wavepackets with respect to pump pulse. (*a*) Two 252 μm BBO crystals placed side by side. (*b*) Two 252 μm BBO crystals interspersed by a 1.545 mm quartz spacer. (*c*) Two 254 μm BBO crystals interspersed by a 308 μm calcite spacer.

thus, the required quartz spacer to BBO crystal thickness ratio is 6.1. Note that the orientation of the birefringent spacer is important; we assume that the quartz spacer is oriented so that an extraordinary ray in the crystal experiences the extraordinary index of refraction in quartz. Figure 2 shows a timing diagram corresponding to such a BBO-quartz-BBO assembly (with crystal thickness $L = 252\,\mu\text{m}$ and spacer thickness $h = 1545\,\mu\text{m}$). The figure indicates, for each location in the crystal sequence, the delay between the signal/idler wavepackets and the pump pulse (for the central PDC wavelength and assuming that the photon pair was created at a specific point of the crystal assembly, as shown). Figure 2(*a*) shows the case of two crystals ($L = 252\,\mu\text{m}$) placed side by side and the timing characteristics for a photon pair generated in the centre of the first crystal. As expected, the signal-idler group delay increases linearly upon transmission. In figure 2(*b*) we show the effect of introducing a quartz spacer ($h = 1545\,\mu\text{m}$) between the two crystals: the signal-idler group delay on the outgoing surface of the second crystal is now identical to that on the outgoing surface of the first crystal.

Figure 3 shows the JSA and JTI functions for the above BBO-quartz-BBO sequence. Figure 3(*a*) shows the PMF for a single BBO crystal (cut angle

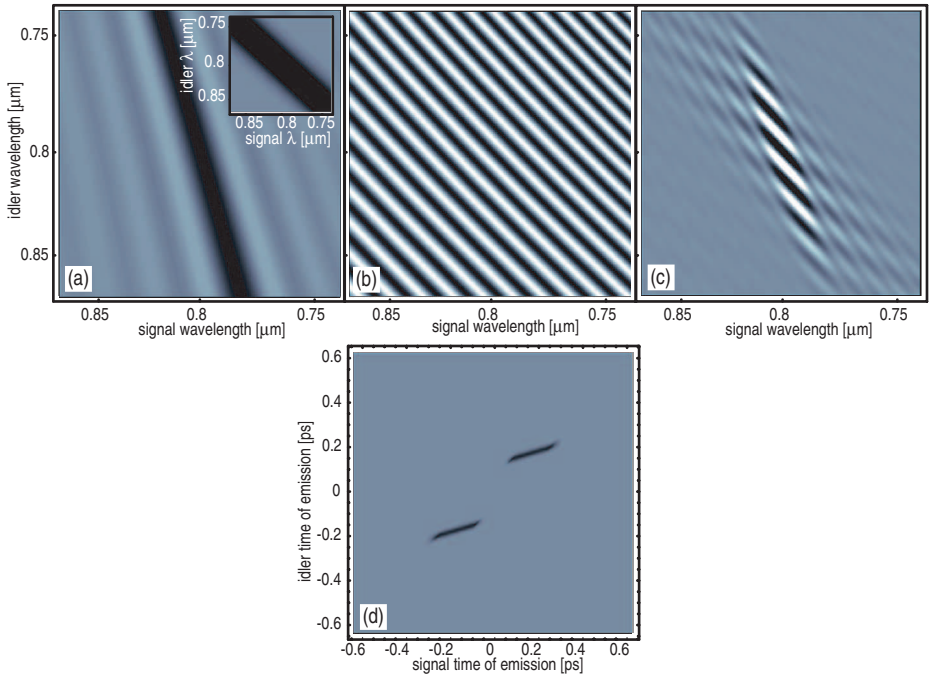

Figure 3. (*a*) PMF for a single BBO crystal; inset shows the PEF with a 8 nm bandwidth. (*b*) The sequence contribution resulting from the combined BBO-quartz dispersion. (*c*) Product of the preceding three functions yielding the JSA. (*d*) Resulting JTI.

$\theta_{PM} = 42.35^{\circ}$; thickness $L = 252\,\mu\text{m}$). Figure 3(*b*) shows the sequence contribution resulting from the combined BBO and quartz dispersion. Note that the cosine term in equation (6) yields a spectral modulation along $\omega_s + \omega_i$. Figure 3(*c*) shows the JSA resulting from the product of the single crystal PMF, the sequence contribution and the PEF (8 nm bandwidth), shown in the inset of (*a*). Figure 3(*d*) shows the JTI (calculated numerically as the modulus squared of the 2D FFT of the JSA). Note that the JTI consists of the coherent sum of two amplitudes, temporally offset from each other in the $t_s + t_i$ direction. It turns out that the phase relationship between the two amplitudes depends on the spectral phase $h\Delta\kappa^{(0)}/2$ in the cosine term of equation (6). For $h\Delta\kappa^{(0)}/2 = \pi j$ with integer j, the spectral modulation is cosine-like, resulting in the two amplitudes being in phase with respect to each other. For $h\Delta\kappa^{(0)}/2 = \pi j + \pi/2$ with integer j, the spectral modulation is sine-like, resulting in the two amplitudes being out of phase. The resulting state may be regarded as a multimode time-bin Bell state of the form:

$$|\phi^{\pm}\rangle = \frac{1}{\sqrt{2}} \iint dt_a dt_b \Big[\tilde{g}(t_1, t_1; t_a, t_b) |t_1 + t_a\rangle_H |t_1 + t_b\rangle_V \pm \tilde{g}(t_2, t_2; t_a, t_b) |t_2 + t_a\rangle_H |t_2 + t_b\rangle_V \Big] \tag{8}$$

where the function $\tilde{g}(t_x, t_y; t_a, t_b) = \tilde{g}(t_a - t_x, t_b - t_y)$ represents one of the two amplitudes, centred at times $\{t_x, t_y\}$ and H/V refer to the horizntal/vertical polarizations. The two amplitudes shown in figure 3(*d*) and described in equation (8) can be interpreted in terms of two 'time-bins' t_1 and t_2, each with a width determined by the function $\tilde{g}(t_1, t_1; t_a, t_b)$. Note that for delta-like $\tilde{g}$ functions, the resulting single-mode state becomes $|\phi^{\pm}\rangle = 2^{-1/2}(|t_1\rangle_H|t_1\rangle_V + |t_2\rangle_H|t_2\rangle_V)$. The state in equation (8) can be thought of as a superposition of multiple such single-mode time-bin Bell states. Note that the time-bin entanglement is also apparent in figure 2, where the amplitudes for photon pair emission from each of the crystals are offset from each other by a time resulting from the combined quartz-BBO dispersion. Note further that by splitting the two polarizations, e.g. by placing a polarizing beam-splitter after the PDC source, the polarization subscripts $\{H, V\}$ are mapped to spatial mode subscripts $\{1, 2\}$; the state in equation (8) becomes essentially equivalent to that produced by the double pump pulse scheme developed by Gisin and co-workers [9–13]. It should be noted that the role played by the different signal and idler photon frequencies (using non-degenerate PDC) in Gisin's scheme, is played here by orthogonal polarizations in type-II PDC. It should also be noted that the time delay between time-bins is introduced here by the birefringence of the crystal assembly, and is in general in the region of femtoseconds; in Gisin's work the time bins are defined by two arms of an interferometer which can provide a much longer (in the region of ns) delay between time bins. It should also be noted that, in contrast with Gisin's scheme, our scheme is capable of producing all four Bell states without recourse to time-non-stationary devices. In order to transform the state from $|\phi^+\rangle$ to $|\phi^-\rangle$ or vice versa, the spacer thickness must be altered by an incremental thickness (see equation 6) thus switching between cosine-like and sine-like behaviour:

$$\Delta h = \frac{\pi}{\Delta\kappa^{(0)}}. \tag{9}$$

For a BBO-quartz-BBO sequence, Δh has a value of 8.18 μm. A possible approach to modifying the spacer thickness on the order of Δh (see equation 9) is using a translatable wedged spacer. It should be pointed out that Δh is small enough that the h/L ratio, crucial for maintaining the desired GVM behaviour, does not change appreciably in switching between $|\phi^+\rangle$ and $|\phi^-\rangle$.

The second of the GVM scenarios described above corresponds to $\tau_+ = 0$ and requires: (i) the quantities $k'_s + k'_i - 2k'_p$ and $\kappa'_s + \kappa'_i - 2\kappa'_p$ to exhibit opposite signs and (ii) the thicknesses L and h to be chosen appropriately so that $\tau_+ = 0$ (see equation 5). This condition can be realized experimentally by a pair of BBO crystals and a calcite spacer: while BBO exhibits $k'_s + k'_i - 2k'_p = -354$ fs/mm, calcite exhibits $\kappa'_s + \kappa'_i - 2\kappa'_p = 294$ fs/mm (at 800 nm); thus, the required calcite spacer to BBO crystal thickness ratio is 1.204. Figure 2(*c*) shows the corresponding timing diagram where we assume $L = 254$ μm and $h = 309$ μm. The timing behaviour for a photon pair generated in the centre of each of the two crystals is shown. Note that the photon pair generated in the first crystal is symmetrically delayed with respect to the pump in the centre of the second crystal, as expected from the condition $\tau_+ = 0$. The fourth element shown is a birefringent medium which delays the signal relative to the idler in order to overlap the contributions from

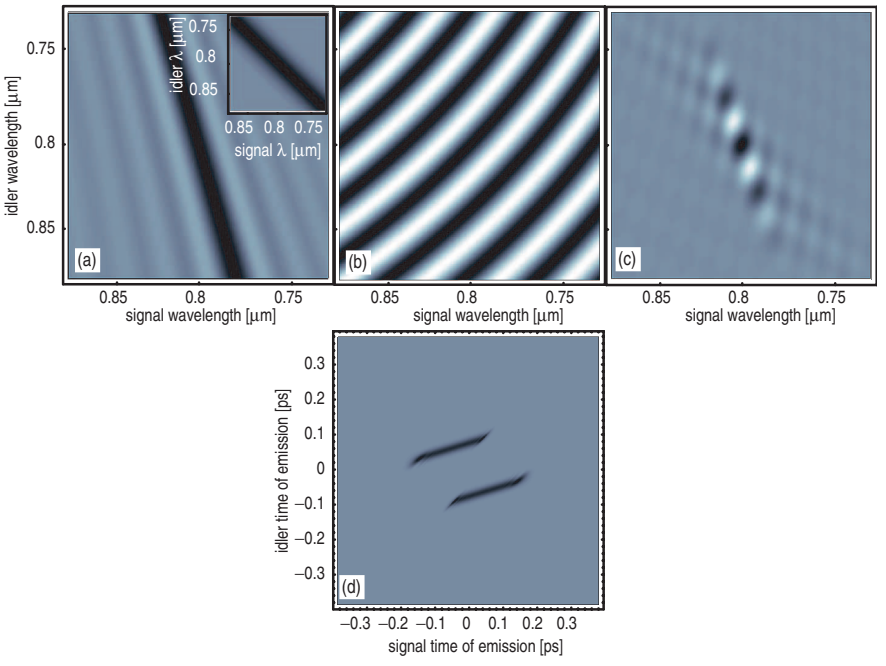

Figure 4. (*a*) PMF for a single BBO crystal; inset shows the PEF (8 nm bandwidth). (*b*) The sequence contribution resulting from the combined BBO-calcite dispersion. (*c*) Product of the preceding three functions yielding the JSA. (*d*) The resulting JTI.

the two crystals: at the end of the structure, the e-ray wavepacket from crystal 1 overlaps the o-ray wavepacket from crystal 2, and vice versa. For graphic clarity, a material exhibiting $k'_s - k'_i = 953\,\text{fs/mm}$ (30 times the quartz value) is assumed with thickness $L_d = 146\,\mu\text{m}$; in practice such a delay can be introduced either with a realistic birefringent crystal such as quartz (requiring a 4.39 mm length) or by a polarization dependent delay line.

Figure 4 shows the JSA and JTI for the BBO-calcite-BBO sequence described above. Figure 4(*a*) shows the PMF for a single BBO crystal. Figure 4(*b*) shows the sequence contribution resulting from the combined BBO and calcite dispersion. Note that the cosine term in equation (6) yields a spectral modulation along $\omega_s - \omega_i$. Figure 4(*c*) shows the joint spectral amplitude resulting from the product of the single crystal PMF, the sequence contribution and the PEF (8 nm bandwidth assumed), shown in the inset of (*a*). Figure 4(*d*) shows the JTI which consists of the coherent sum of two amplitudes, temporally offset from each other in the $t_s - t_i$ direction. The state thus produced may be regarded as a multimode time-bin Bell state of the form:

$$|\psi^{\pm}\rangle = \frac{1}{\sqrt{2}} \iint dt_a dt_b \Big[\tilde{g}(t_1, t_2; t_a, t_b) |t_1 + t_a\rangle_H |t_2 + t_b\rangle_V \pm \tilde{g}(t_2, t_1; t_a, t_b) |t_2 + t_a\rangle_H |t_1 + t_b\rangle_V \Big]. \tag{10}$$

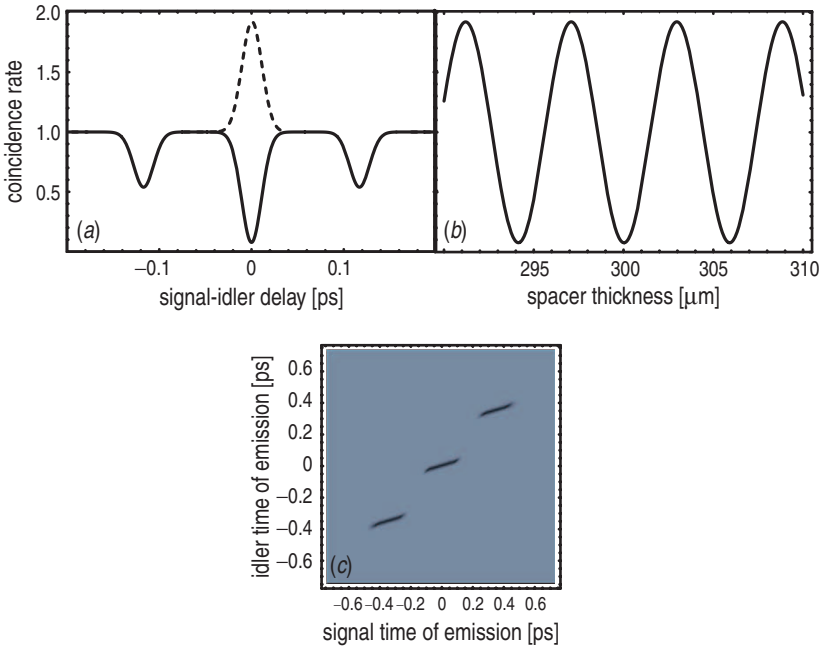

Figure 5. (*a*) Coincidence rate functions for the BBO-calcite-BBO sequence showing (solid line) the case of a $|\psi^+\rangle$ state and (dashed lined) a $|\psi^-\rangle$ state. (*b*) The coincidence rate function evaluated in the centre of the interference pattern as a function of the calcite spacer thickness. (*c*) Qutrit state synthesized by a BBO-quartz sequence with three crystals and two spacers.

For clarity, we point out that for delta-like $\tilde{g}$ functions, the resulting single-mode state becomes $|\psi^{\pm}\rangle = 2^{-1/2}(|t_1\rangle_H|t_2\rangle_V + |t_2\rangle_H|t_1\rangle_V)$.

As is well known, a Hong–Ou–Mandel (HOM) interferometer can be used to discriminate between the singlet state $|\psi^-\rangle$ and the remaining three Bell states. While $|\psi^-\rangle$ yields a unit coincidence rate (at the centre of the resulting interference pattern) following from its fermionic antisymmetry, $|\psi^+\rangle$, $|\phi^+\rangle$ and $|\phi^-\rangle$ yield a null coincidence rate. We thus expect that by modifying the spacer thickness by multiples of the incremental thickness Δh, the resulting interference in a HOM interferometer should oscillate between a dip and a peak corresponding to the two extrema $|\psi^+\rangle$ and $|\psi^-\rangle$. Figure 5(*a*) shows theoretical coincidence rate functions (as a function of signal-idler delay, calculated as in [8]) exhibiting the expected behaviour with $\Delta h = 2.44\,\mu\text{m}$. Note that the interference curve exhibits two satellite dips which occur at delay settings such that time-bin t_1 in the signal photon interferes with time-bin t_2 in the idler photon, or vice versa; for the central peak/dip, both signal time-bins interfere with both idler time-bins. Figure 5(*b*) explicitly shows the oscillation between $|\psi^+\rangle$ and $|\psi^-\rangle$ behaviour as a function of the spacer thickness. Note that the interference visibility is not perfect (i.e. for the $|\psi^+\rangle$ state the coincidence rate does not reach zero and for the $|\psi^-\rangle$ it does not reach 2). The former is due to spectral distinguishing information inherent in type-II PDC [8]; in general the visibility drops with crystal (and spacer) length.

It should be pointed out that with this system it is straightforward to produce higher dimensionality states, such as arbitrary qutrits and in general qudits. For example, in the case of the BBO-quartz-BBO sequence discussed above, adding one more spacer and crystal (i.e. total of three crystals and two spacers), results in a qutrit state of the form $|\psi\rangle = 3^{-1/2}(|t_1\rangle_H|t_1\rangle_V + |t_2\rangle_H|t_2\rangle_V + |t_3\rangle_H|t_3\rangle_V)$; see figure 5(*c*). The flexibility afforded by this technique is likely to make it a useful technology for the design of specific states for the growing field of quantum information processing.

In summary, we have shown that tailored group velocity matching via type-II PDC crystal pairs interspersed with birefringent compensators can yield time-bin entangled states. All four Bell states can thus be generated without resorting to time non-stationary devices such as a Pockels cells. In particular, matching the signal to the idler, which can be accomplished with a BBO-quartz-BBO sequence, yields the $|\phi^{\pm}\rangle$ Bell states, while matching the PDC photons to the pump pulse, which can be accomplished with a BBO-calcite-BBO sequence, yields the $|\psi^{\pm}\rangle$ states. By using longer crystal sequences, with multiple crystals and spacers it is possible to generate more complicated states such as time-bin qudits with specific properties.

References

[1] T.E. Keller and M.H. Rubin, Phys. Rev. A **56** 1534 (1997).
[2] W.P. Grice, A.B. U'Ren and I.A. Walmsley, Phys. Rev. A **64** 063815 (2001).
[3] V. Giovannetti, L. Maccone, J.H. Shapiro, *et al.*, Phys. Rev. A **66** 043813 (2002).
[4] O. Kuzucu, M. Fiorentino, M.A. Albota, *et al.*, quant-ph/0410216 (2004).
[5] A.B. U'Ren, K. Banaszek and I.A. Walmsley, Quant. Inform. Comput. **3** 480 (2003).
[6] A.B. U'Ren, Ch. Silberhorn, K. Banaszek, *et al.*, Laser Phys. **15** 146 (2005).
[7] A.B. U'Ren, R. Erdmann, M. de la Cruz-Gutierrez and I.A. Walmsley, unpublished.
[8] W.P. Grice and I.A. Walmsley, Phys. Rev. A **56** 1627 (1997).
[9] R.T. Thew, S. Tanzilli, W. Tittel, *et al.*, Phys. Rev. A **66** 062304 (2002).
[10] I. Marcikic, H. de Riedmatten, W. Tittel, *et al.*, Phys. Rev. A **66** 062308 (2002).
[11] I. Marcikic, H. de Riedmatten, W. Tittel, *et al.*, Nature **421** 509 (2003).
[12] H. de Riedmatten, I. Marcikic, W. Tittel, *et al.*, Phys. Rev. Lett. **92** 047904 (2004).
[13] I. Marcikic, H. de Riedmatten, W. Tittel, *et al.*, Phys. Rev. Lett. **93** 180502 (2004).